HEFAT2011
8th International Conference on Heat Transfer, Fluid Mechanics and Thermodynamics
11 – 13 July 2011
Pointe Aux Piments, Mauritius

THERMOGRAPHIC ANALYSIS OF THIN LIQUID FILMS ON A ROTATING DISC: APPROACH AND CHALLENGES

Ghiasy D.*, Boodhoo K.V.K. and Tham M.T.
*Author for correspondence
School of Chemical Engineering and Advanced Materials,
Newcastle University, Newcastle upon Tyne, NE1 7RU, England, U.K
E-mail: dena.ghiasy@ncl.ac.uk

ABSTRACT

This paper examines the temperature profiles and flow characteristics of thin liquid films on a rotating surface by means of an Infrared (IR) thermal imaging camera. The challenges of obtaining accurate temperature measurements using thermographic techniques, in particular for thin liquid films of varying thicknesses, are outlined in this study. The captured images of the liquid film provide a visual insight into the heat transfer mechanism as the cold liquid moves from centre of a rotating disc towards its edges. The effect of liquid film viscosity, rotational speed, feed flowrate and disc temperature on heat transfer efficiency from the heated disc to the cold film is investigated. The temperature profiles obtained by the Infrared camera are compared to those estimated by a theoretical model of disc/film heat transfer. The results provide an excellent platform for qualitative analysis of heating thin liquid films in highly accelerated centrifugal fields. The quantitative analysis is, however, associated with some degrees of uncertainty due to the limitations described in this paper.

INTRODUCTION

The spinning disc reactor (SDR) is a classical example of successful process intensification which offers enhanced mixing and heat/mass transfer performances [1-5]. Processing film and disc temperatures are typically measured by thermocouples inserted through the rotating shaft via a slip ring assembly. Measuring the film temperature by this invasive technique requires the thermocouple to protrude through the film which may disturb the continuous flow of fluid, especially in the presence of a very thin film at the measuring point on the disc. Further, due to certain design limitations in some SDRs, the only temperature measurements available are provided by thermocouples immersed in the heat transfer fluid whereby the film temperature has to be inferred from such indirect measurements. In this study an IR thermal imager, which is capable of producing temperature measurements in a non-contact mode, was used to shed light on the SDR heat transfer capability and processing film temperature profiles.

NOMENCLATURE

C_p	[J/kgK]	Specific heat capacity
h	[W/m^2 K]	Film heat transfer coefficient
k	[W/mK]	Thermal conductivity
m	[kg/s]	Mass flowrate
N	[rpm]	Rotational speed
Q	[m^3/s]	Volumetric flowrate
r	[m]	Radial distance from the disc centre
T	[K]	Temperature
W	[W]	Radiation power

Special characters

α	[-]	Absorptance
ε	[-]	Emissivity
ρ	[-]	Reflectance
τ	[-]	Transmittance
υ	[m^2/s]	Kinematic viscosity
ω	[rad/s]	Angular velocity ($2\pi N/60$)
δ	[m]	Film thickness

Subscripts

atm	Atmosphere
d	Disc
f	Feed
i	Inlet
obj	Object
refl	Reflection
tot	Total

Apparatus

The general operating principle of SDRs is based on generating high acceleration environments by rotating a disc surface, which in this study is a smooth stainless steel horizontally mounted plate (16 cm diameter), as shown in Figure 1. The liquid feed streams are pumped into a well in the centre of the top surface of the disc. As the disc rotates the well acts as a reservoir system to enable uniform distribution of the feeds across the disc surface. Under the action of high centrifugal fields, the liquid travels rapidly towards the disc edges and forms a very thin, highly sheared film typically covered with numerous surface ripples. At the disc periphery the liquid is thrown out and hits the stationary walls of the reactor housing.

The disc contains internal channels for flow of a heat transfer fluid, providing heating or cooling. The heat transfer

fluid is delivered to the centre of the bottom surface of the disc through an internal pipe within the rotation shaft. The heating/cooling fluid moves towards the disc edges and exits the chamber before it gets recirculated through the system via a temperature controlled heat transfer unit, as schematically shown in Figure 2. The disc temperature is inferred from two thermocouples inserted in the inlet and outlet heat transfer fluid pipes to the SDR unit. At steady state conditions the stainless steel disc with high thermal conductivity is expected to reach the temperature of the heat transfer fluid flowing in the narrow channels underneath the disc. This was confirmed by the thermal images of the dry disc. The mass of processing fluid on the disc at any one time is very small in comparison with the mass of the disc, thus the amount of heat transferred to the thin liquid film is not significant enough to cause any large variations in temperatures across the disc. Therefore the disc temperature was taken to be uniform and equal to the heat transfer fluid flowing underneath the disc.

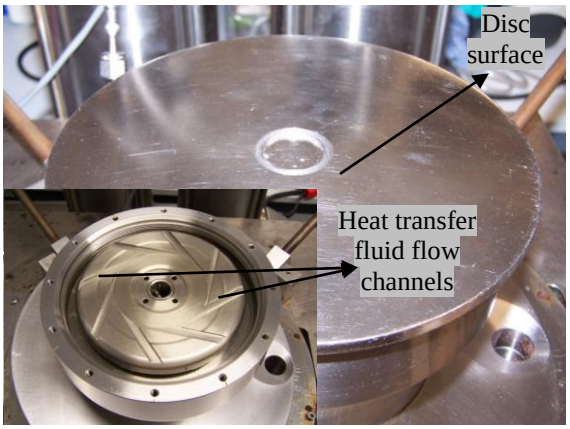

Figure 1 View of disc surface and internal heat transfer channels

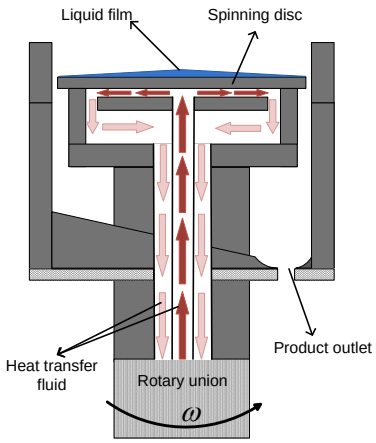

Figure 2 Schematic of SDR

The thermal imager used in this study is a FLIR ThermaCAM SC640 which is a long wave band (7-13μm), capable of real time scanning and analysis, or the capture of images at up to 30 frames per second for subsequent analysis. A 19mm/45° IR lens was used to capture the images. The camera was connected to a laptop via a firewire cable which allowed remote operation. The analysis of the captured images, including the conversion to other formats such as Excel, was carried out using the ThermaCAM Researcher Pro 2.10 software. The camera was fixed to a support structure above the SDR unit as shown in Figure 3.

The main disadvantage of the current setup is that the liquid film is exposed to an open environment, which will result in heat loss from the liquid film to the surrounding air through convection and possibly evaporation. As part of the design, a reactor lid made of a material transparent to IR radiation was considered, in order to enclose the system and ensure a saturated environment in equilibrium with the liquid film on the disc exists. This objective, however, did not materialise due to cost factors and technical difficulties involved in machining the feed inlet tubes on a specialised IR transparent material. It should be noted that materials such as glass and Perspex, which are transparent to visible light, are infrared opaque.

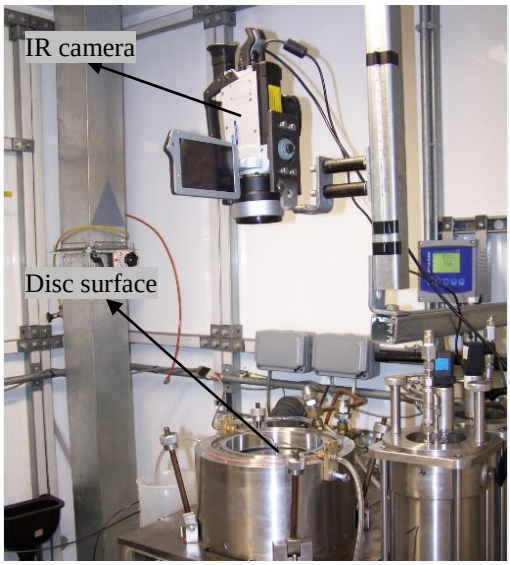

Figure 3 Apparatus setup

THEORY OF THERMOGRAPHY

Thermal imaging cameras detect infrared radiation and produce a visual image, referred to as a thermogram, which depicts the thermal variations within the object being measured. All objects emit IR at temperatures above absolute zero and the amount of radiation increases with temperature. Thermography is applied in a wide variety of different fields such as military and security services, building and infrastructure, research and industry, as well as medical applications and many more.

Thermographic Measurements

The IR camera receives radiation from the object being measured, plus radiation from its surroundings reflected onto the target object's surface. These radiation components are attenuated to some extent as they pass through the atmosphere due to absorption by gases and scattering by particles. Since the

atmosphere can absorb part of the radiation energy it can also radiate some itself. This situation is illustrated in Figure 4.

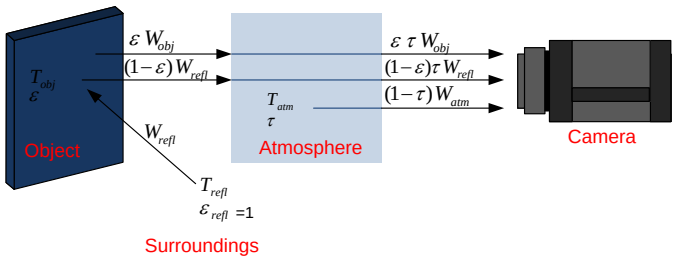

Figure 4 Schematic of the general thermographic measurement (adopted from ref. [6])

The total radiation power received by the camera is given by:

$$W_{tot} = \varepsilon\tau W_{obj} + (1-\varepsilon)\tau W_{refl} + (1-\tau)W_{atm} \qquad (1)$$

The above equation is the basis of the general measurement formula used by all the FLIR systems.

The following object parameters must be supplied to the camera used in this study (FLIR SC640) in order to compensate for the effect of a number of different radiation sources:

1. The emissivity of the object.
2. The reflected apparent temperature.
3. The distance between the object and the camera
4. The relative humidity.
5. Temperature of the atmosphere.

The accuracy of the object temperature estimated by the camera is often closely linked to the accuracy of evaluation of the above input parameters. The emissivity value of the object is typically the most important parameter which needs to be determined accurately. The accuracy of the input parameters becomes less critical if the target object has high emissivity and is significantly hotter than its surroundings.

Emissivity

Emissivity, typically denoted by ε, is a measure of how much radiation is emitted from the object, compared to that from a blackbody[1] of the same temperature. Theoretically, emissivity values range from 0 to 1. Energy conservation requires that any radiation incident on any object is either reflected, transmitted or absorbed, thus:

$$\rho + \tau + \alpha = 1 \qquad (2)$$

Where ρ, τ and α denote fractions of radiation that is reflected, transmitted and absorbed respectively. Kirchhoff's law states that the amount of radiation absorbed by any object is equal to the amount of radiation that is emitted by that object (i.e. $\varepsilon = \alpha$), therefore:

$$\varepsilon = 1 - \rho - \tau \qquad (3)$$

For opaque solids ($\tau = 0$) emissivity can be estimated if the total reflectivity of the object is known. Emissivity is affected by the parameters listed below [7] :

1. Material (metals/non-metals): a non-metal emitter is often a graybody[2] with emissivity values typically above 0.8. Metals are generally highly reflective and exhibit low values of emissivity, often below 0.2.
2. Surface condition (rough/ polished): polished surfaces may have emissivity values as low as 0.02, whilst the emissivity of the same material but with a roughened surface can be much higher.
3. Regular geometry (grooves, cavities, etc.): Regular surface structures increase the value of emissivity.
4. Viewing angle: an object which is observed from a direction perpendicular to its surface has higher emissivity than when observed at oblique angles.
5. Wavelength: the emissivity of metals usually decreases with wavelength, whereas non metals can show increases as well. Narrow band filters can be used for substances that have wavelength-dependent emissivity.
6. Temperature: emissivity usually varies with temperature.

A study of infrared characteristics of thin polymer films [8] showed that emissivity is also dependent on film thickness (increases with increasing film thickness). The same pattern was also observed for several thin films applied to a stainless steel surface at cryogenic temperatures [9], as illustrated in Figure 5.

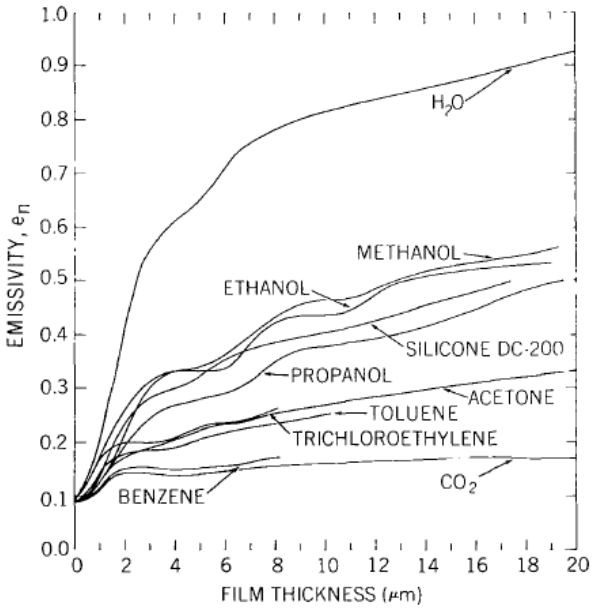

Figure 5 Emissivity as a function of film thickness on polished stainless steel at 77K [9]

[1] A blackbody is an object that absorbs all radiation that impinges on it at any wavelength and has a theoretical emissivity of 1.

[2] A graybody is a non-selective emitter with constant emissivity at any wavelength.

Accurate temperature measurements using an IR camera requires accurate knowledge of the object's emissivity value. Emissivity values for common materials are available in literature; however, these values refer to specific measurement conditions and should therefore be used with caution. Emissivity can directly be measured using several techniques [7]. The easiest method is to attach tape or paint of known emissivity to the object being measured. The object's emissivity value can be found by varying ε in the camera software until the object's temperature matches the known surface temperature of the tape/paint, assuming the temperature distribution across adjacent surfaces is uniform and a thermal equilibrium between the tape/paint and the object under study is reached; this method is, however, only applicable to solid surfaces. Pyrolaser and Pyrofiber [10] infrared thermometer instruments are capable of real time emissivity measurement by measuring the target's diffuse reflectivity.

Errors and uncertainties

Sources of errors can be categorised into three groups [11]:

1. Method: resulting from incorrect evaluation of input parameters such as object's emissivity, atmospheric temperature, relative humidity, etc.
2. Calibration: errors can result from different measurement conditions for the calibration data and each experiment, such as different camera to object distance. Accuracy of the reference standard, number of calibration points and interpolation can also influence the accuracy of final temperature measurement.
3. Electronic path: such as detector noise.

Incorrect setting of the object emissivity is commonly known as the main factor leading to significant temperature measurement errors.

EXPERIMENTAL WORK

The disc/film heat transfer performance was assessed for a range of operating conditions and working fluids, as outlined in Table 1. Some of the data acquired within this range, particularly those at low temperatures and low flowrates, were inversely influenced by the reflection from the surrounding environment.

Table 1. Operating conditions

Working Fluid	T_d *[°C]*	*Q [ml/s]*	*N [rpm]*
Water	25, 50, 70	5, 10, 15, 20	500, 1250, 2000
50%Water 50% Glycerol v/v	25, 70	5, 10	500, 2000
Oil (Therminol SP)	25, 70, 100	1, 5, 10, 15, 20	500, 1250, 2000

Evaluation of Input Parameters

1) Object's emissivity

In this study, the object's emissivity is the most important parameter to be evaluated. The true emissivity of the liquid film on a rotating disc could not be measured in this study and had to be estimated from relevant information available in the literature. The challenge in evaluating the emissivity of thin liquid films on a rotating surface is the fact that emissivity is a function of film thickness, as discussed previously. Theoretical predictions of the liquid film thickness on the spinning disc under a range of operating conditions may be obtained from equation 4, as established in previous research on SDRs [12]:

$$\delta = \left(\frac{3Q\nu}{2\pi\omega^2 r^2} \right)^{1/3} \tag{4}$$

The above equation shows that film thickness decreases as the liquid moves from the disc centre towards the disc edges, as illustrated graphically in Figure 6 and Figure 7 for a number of flowrates and rotational speeds (viscosities evaluated at 43 °C). This relationship implies that the emissivity of the liquid film varies depending on the radial position on the disc.

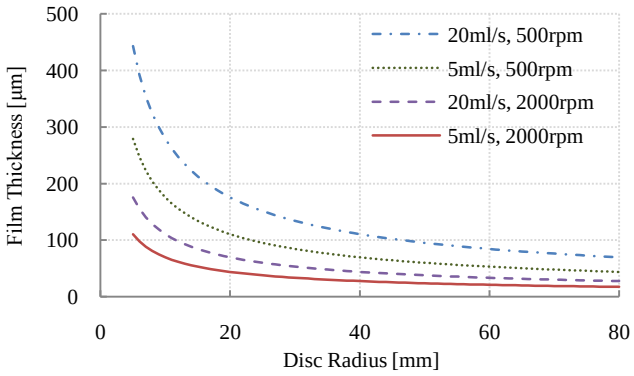

Figure 6 Water film thickness profile, T_d= 70°C, T_f=15°C

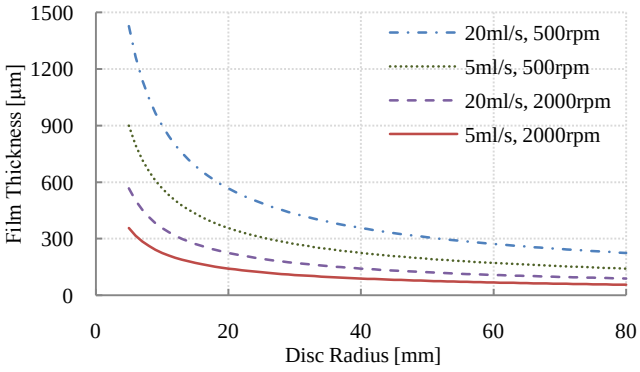

Figure 7 Therminol SP film thickness profile, T_d= 70°C, T_f=15°C

For runs with water, the minimum film thickness was kept above 20 µm. Assuming that the data presented in Figure 5 is applicable to the operating conditions in this study, the emissivity of the water films should not be far from the typical

value of 0.96 [13]; this value was used for runs with water and water-glycerol. However, no data regarding the emissivity of Therminol SP (mixture of synthesis hydrocarbons) were available. The closest information that could be adopted was the emissivity of lubricating oil on Ni base at 20°C, presented in Table 2. Figure 8 illustrates the effect of the minimum and maximum emissivity values taken from Table 2 on temperature measurements across a thin film of Therminol SP for a typical run. It can be seen that the emissivity values significantly influence the temperature measurements, thus accurate measurements are only possible if the emissivity can be determined accurately.

Table 2. Emissivity of lubricating oil [13]

Film Thickness [μm]	*Emissivity*
25	0.27
50	0.46
125	0.72
Thick coating	0.82

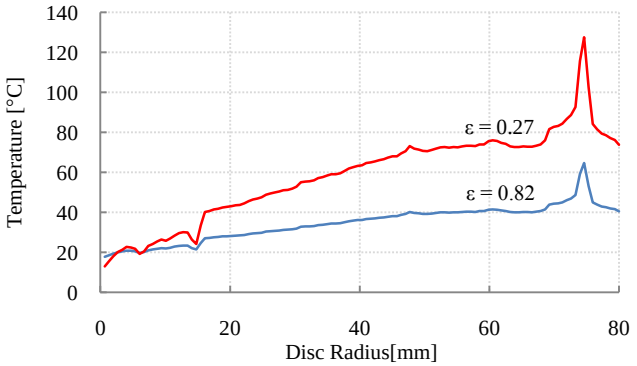

Figure 8 Effect of emissivity on temperature measurement, T_d=70°C

The best way for calculating the temperature profiles across the disc in this study might be to divide each thermogram into a number of small segments and evaluate the corresponding film thickness and emissivity within each segment. A simpler method is to use the value of emissivity corresponding to the estimated average film thickness for each run. The temperature measurements obtained using these two methods for a typical run are illustrated in Figure 9. Using emissivity values corresponding to small segments across the disc is more accurate; however, the difference between the two methods is relatively small. Hence, for simplicity it was decided to use the emissivity values corresponding to the predicted average film thickness for each run.

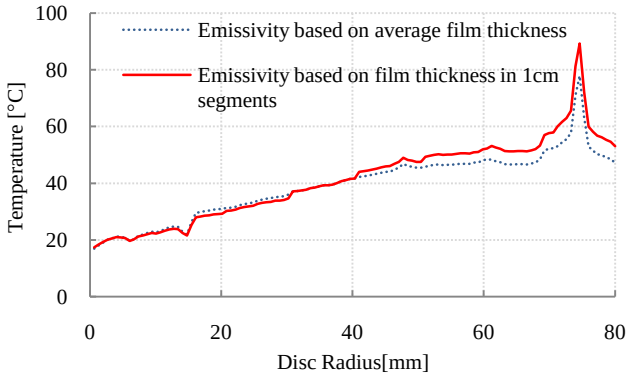

Figure 9 Methods of evaluating emissivity

The underlying limitation, however, is that accurate estimation of film thickness may not be possible as film thickness is a function of kinematic viscosity which is in turn a function of temperature (an unknown parameter). The dependence of viscosity on temperature is especially relevant to relatively viscous process liquids such as Therminol SP used in this study (see Appendix). Furthermore, the presence of surface waves and disturbances due to bringing the liquid up to the disc angular velocity leads to very complex fluid dynamics on the rotating disc, not accounted for in equation 4, which applies to a smooth film. All of these effects make prediction of the true film thickness very difficult across the whole of the disc surface. Consequently, the emissivity values and the resulting temperature measurements are associated with a degree of uncertainty. A simulation investigation of errors in infrared thermography [11] revealed that overestimation of emissivity by 30% leads to – (1 – 4)% error in the measured temperature; whilst underestimation of the emissivity by 30% results in + (2 – 7)% error in the measured temperature for emissivity range of 0.4 to 0.98 and object temperature range of 300 to 400K.

2) The reflected apparent temperature was measured to be 20°C using the procedure described in the camera's user manual.

3) The distance between the object and the camera lens was 0.4 m.

4) For short distances and normal humidity, the relative humidity can generally be left at a default value of 50%.

5) The temperature of the atmosphere was monitored over the run period and an average value of 20°C was measured.

TRENDS AND RESULTS

Temperature profiles

The following mathematical model was developed [14] to predict the temperature profile in thin liquid films across a rotating disc:

$$T = T_d - \frac{(T_d - T_i)}{\exp\{\frac{\pi h}{m c_p}(r^2 - r_i^2)\}} \quad (5)$$

The local heat transfer coefficient, h, may be estimated using the following expression on the basis of the simple Nusselt theory [4]:

$$h = \frac{5k}{3\delta} \qquad (6)$$

The physical properties required to estimate the theoretical temperature profile were evaluated at a temperature of ½ (disc temperature + liquid feed temperature). The physical properties of Therminol SP were provided by the manufacturer, as shown in the Appendix, whilst the physical properties of water were obtained from NIST Chemistry WebBook.

Figure 10 and Figure 11 show the typical temperature profiles of thin water films across the disc, both measured by the IR thermal imager and predicted form the mathematical model. As can be seen, the temperature profiles obtained from the thermographic measurement are significantly lower than those predicted by the theoretical expression. One of the main assumptions in deriving equation 5 is that heat losses to the surroundings are negligible. However, as in this practical set-up the liquid film was exposed to relatively cold air at 20°C and a saturated environment in equilibrium with the liquid film did not exist, the validity of this assumption needs to be verified. Assuming that Wagner's approach [15] for calculating the heat transfer coefficient from a rotating disc to ambient air is applicable for the case of heat transfer from a laminar flow liquid film to the surrounding air, the convective heat loss may be estimated. The heat loss due to convection using this approach was found to be less than 3% of the total heat input, which can be considered negligible. This agrees well with Quinn and Cetegen's [16] analysis which revealed that the heat loss due to convection into the air above the disc was at most 1% of the overall heater power. The assumption of negligible heat loss to the surroundings could also be undermined due to potential evaporation from the liquid film. Quinn and Cetegen [16] conclude that evaporative cooling from the liquid film surface only has a moderate effect on the Nusselt number magnitude. However, this effect should be accounted for in the theoretical model in order to enable a closer comparison between theory and experimental data. Another assumption in deriving equation 5 is that the thickness of the film is so small and mixing within the film is so intense that temperature variations across the height of the film are negligible. If this assumption is not valid, the surface of the liquid film which is measured by the IR camera is expected to be at a lower temperature than the liquid layer in contact with the disc. The rather large discrepancy between the theoretical and measured film temperatures could be attributed to a combination of factors such as underlying assumptions of the model not being valid in practice and also errors in measured temperatures due to incorrect emissivity values. Valid comparison between the IR thermographic measurements and a theoretical model may only be possible if uncertainties in evaluation of emissivity of thin films with varying thickness could be removed and also a more vigorous mathematical model is developed which accounts for convective and evaporative heat losses as well as variation of temperature in the axial direction.

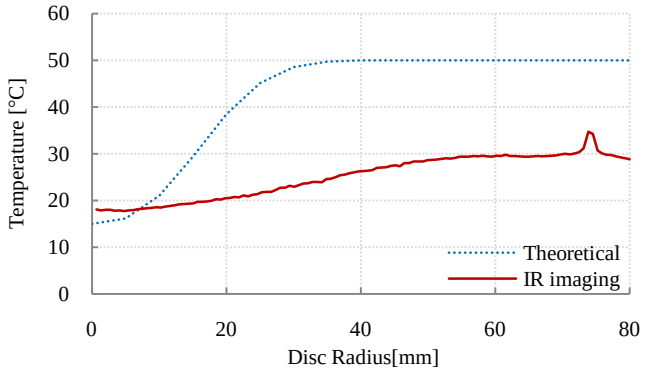

Figure 10 Q = 5 ml/s, N = 2000 rpm, T_d=50°C, working fluid: Water

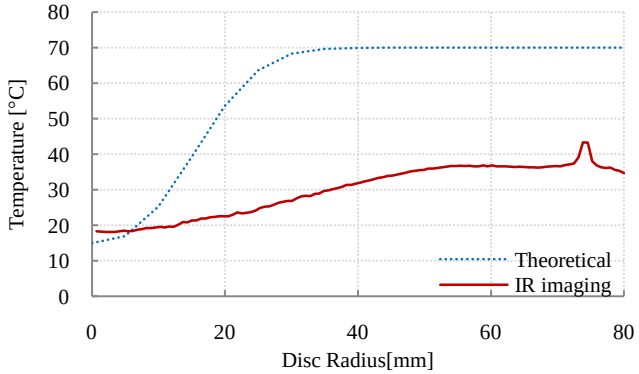

Figure 11 Q = 5 ml/s, N = 2000 rpm, T_d=70°C, working fluid: Water

Figure 12 and Figure 13 show the theoretical and thermographic temperature profiles in thin oil films across the rotating disc for a typical run. It can be observed that near the disc centre where the film thickness is high, temperatures estimated by the IR camera are higher than those predicted by the mathematical model. Conversely, towards the disc periphery where the liquid film gets thinner temperatures are under-estimated by IR camera compared to the theoretical values. This trend was also observed for the water films but the cross-over point was closer to the disc centre.

Since Therminol SP has a high boiling point of 351°C at atmospheric pressure, it is unlikely that any significant amounts of heat could have been lost due to evaporation. This is reflected by the measured film temperature in Figure 13 approaching the theoretical profile more closely than with water (Figure 11), under identical conditions of operation of the disc. Nevertheless, a certain discrepancy between the theoretical and the experimentally determined temperature profiles still remains, which indicates other factors as discussed earlier may be at play. The sudden increase in temperature detected by the thermal imager near the disc periphery is believed to be caused by metal on metal contact of the disc and the supporting assembly (see Figure 2).

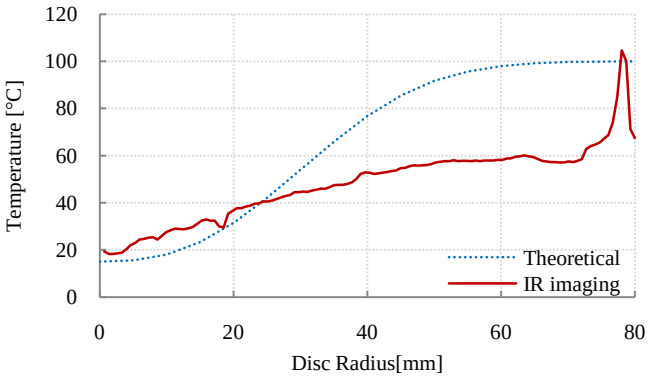

Figure 12 Q = 5 ml/s, N = 2000 rpm, T_d=100°C, working fluid: Therminol SP

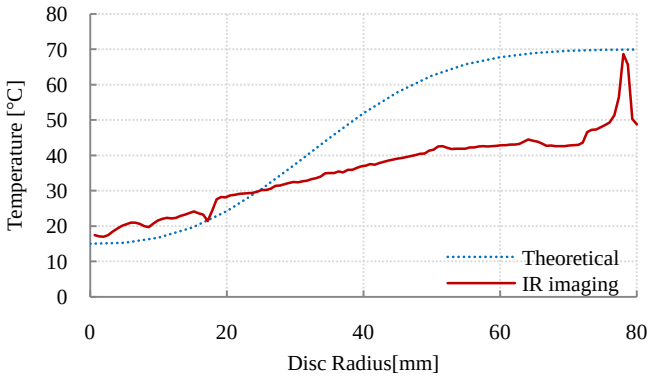

Figure 13 Q = 5 ml/s, N = 2000 rpm, T_d=70°C, working fluid: Therminol SP

Liquid film Characteristics

In addition to temperature profiles, the thermograms obtained in this study depict the liquid film characteristics and wave patterns across the disc due to temperature variations on wavy liquid film surfaces. Figure 14 shows the typical liquid flow profiles of water-like fluids on a rotating disc. At low rotational speeds (Figure 14a), there appears to be a significant number of large amplitude surface waves on the film which result in rather jagged boundaries between different segments of the film as it propagates in an almost radial manner outwards under the influence of the centrifugal force. The waves decay as the film moves towards the disc edges. A faint spiral profile is also apparent in the inner regions of the disc in Figure 14a in contrast to Figure 14b, which is indicative of the retarding Coriolis forces [14, 17] on the film exerting a an increasingly significant influence on the film flow close to the centre of the disc at lower disc speeds. As viscosity of the working fluid is increased by adding glycerol to water (Figure 15), stark differences are observed. The film travels in a more pronounced spiral path which unwinds in the direction of rotation and the surface waves, as observed with water, no longer seem to be present. This effect is due to viscous damping of surface waves which leads to a smoother film being generated.

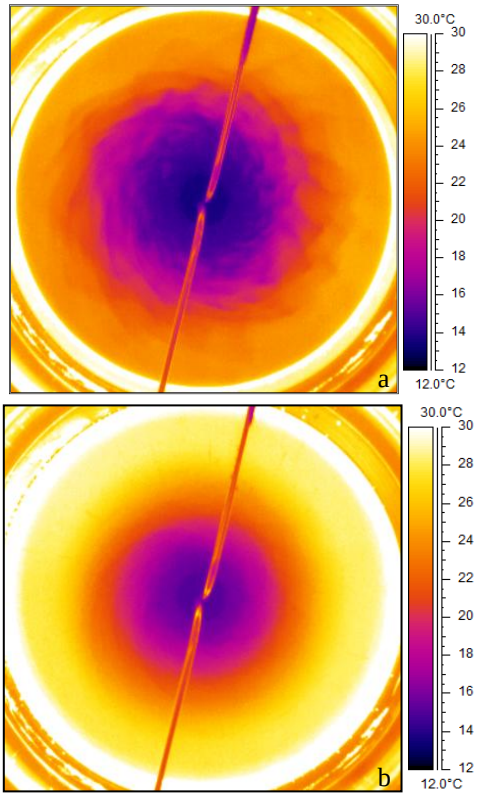

Figure 14 Q = 10 ml/s, working fluid: water, a) N=500 rpm b) N=2000 rpm

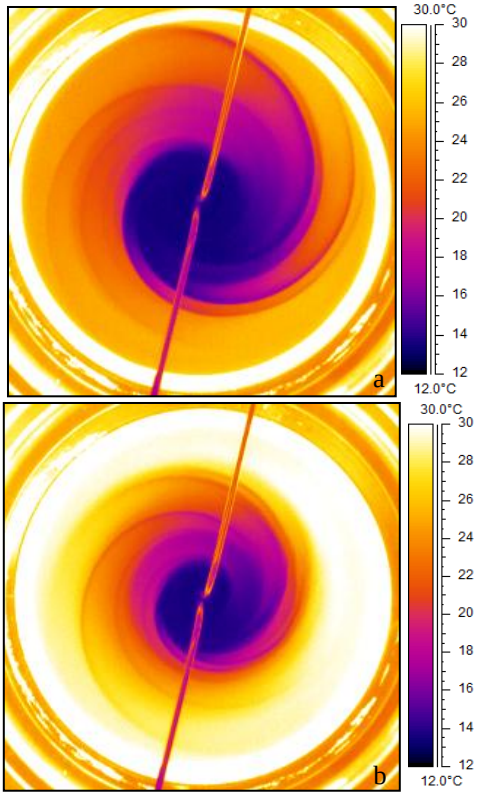

Figure 15 Q = 10 ml/s, working fluid: 50% water 50% glycerol v/v, a) N=500 rpm b) N=2000 rpm

The thermograms presented in both Figure 14 and Figure 15 illustrate that increasing the disc rotational speed at a constant flow rate results in narrowing of the cold central region and thus improved disc/film heat transfer performance. This is attributed to reduced film thickness and thus reduced conduction path with increasing angular velocity.

Figure 16 shows the effect of varying flowrate at constant rotational speed. As expected reducing flowrate at constant angular velocity results in thinner films being formed, therefore, improved heat transfer capability between the disc surface and liquid film resulting in higher temperatures.

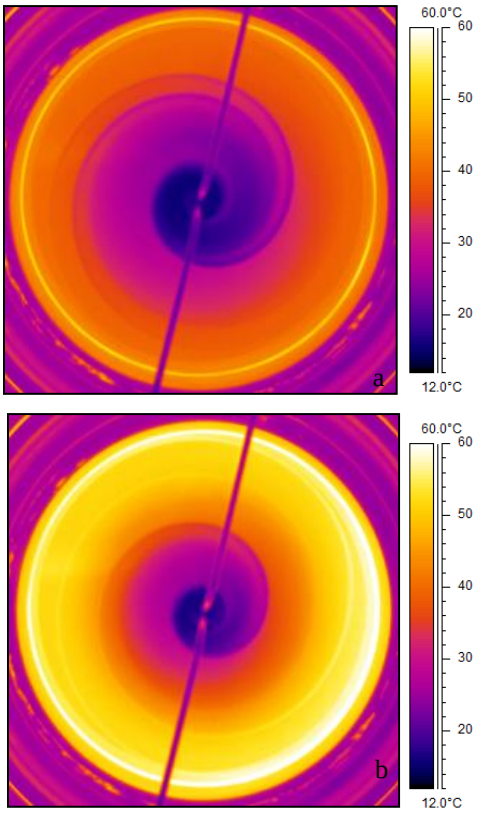

Figure 16 N = 500 rpm, working fluid: Therminol SP, a) Q=10 ml/s b) Q=5 ml/s

CONCLUSIONS

The following challenges and limitations were encountered in the attempted thermographic analysis of thin liquid films on a rotating disc:

1. Limitations in enclosing the spinning disc reactor using a material that is cost effective, transparent to IR radiation and has sufficient mechanical strength for incorporating the two liquid feeds.
2. Accurate temperature measurements are only possible if a number of input parameters, emissivity being the most important one, can be estimated with high accuracy.
3. The emissivity of thin liquid films is a function of film thickness.

The temperature measurements obtained in this study are associated with some levels of uncertainty as the true emissivity of the liquid film on the rotating disc could not be measured. Furthermore, as the liquid film was not in equilibrium with the surrounding environment the measured temperatures do not reflect the actual disc/film heat transfer capabilities.

Aside from reinforcing the challenges and limitations of quantitative thermographic analysis in general and thin liquid films in particular, the following conclusions can be drawn from this study:

1. The flow path and wave characteristics on a rotating disc change significantly as the fluid viscosity increases. These are attributed to Coriolis forces and viscous damping of surface wavelets respectively.
2. The disc/film heat transfer performance is enhanced as the film thickness is reduced at higher disc speeds and/or lower flowrates.

REFERENCES

1. Boodhoo, K.V.K. and R.J.J. Jachuck. Application of the spinning-disc technology for process Intensification in the chemical process industry.*4th International Workshop on Materials Processing at High Gravity*. 2000. Potsdam, Ny: Kluwer Academic/Plenum Publ.
2. Oxley, P., C. Brechtelsbauer, F. Ricard, N. Lewis, and C. Ramshaw, Evaluation of spinning disk reactor technology for the manufacture of pharmaceuticals. *Industrial & Engineering Chemistry Research*, 2000. **39**(7): p. 2175-2182.
3. Yatmaz, H.C., C. Wallis, and C.R. Howarth, The spinning disc reactor - studies on a novel TiO2 photocatalytic reactor. *Chemosphere*, 2001. **42**(4): p. 397-403.
4. Aoune, A. and C. Ramshaw, Process intensification: heat and mass transfer characteristics of liquid films on rotating discs. *International Journal of Heat and Mass Transfer*, 1999. **42**(14): p. 2543-2556.
5. Ramshaw, C. and S. Cook, Spinning around. *The Chemical Engineer*, 2005(774-775): p. 42-44.
6. *FLIR Systems User's Manual: ThermaCAM SC640*. Publ. No: 1558550, Rev: a201, 2007.
7. Vollmer, M. and K.P. Mollmann, *Infrared Thermal Imaging: Fundamentals, Research and Applications*. 2010, Germany: WILEY-VCH.
8. Cao, B., P. Sweeney, and G.A. Campbell. Infrared characteristics of thin polymer film: temperature measurement of polyethylene.*Annual Technical Conference - Society of Plastics Engineers*. 1989. New York, NY, USA: Publ by Soc of Plastics Engineers.
9. Viehmann, W. and A.G. Eubanks, *Effects of surface contamination on the Infrared emissivity and visible-light scattering of highly reflective surfaces at cryogenic temperatures*. Technical Note, 1972, Goddard Space Flight Centre.

10. Kral, J. and E.K. Matthews. *Pyrolaser & Pyrofiber Infrared Temperature Measurement with Automatic Emissivity Correction*.1996 [accessed 2011]; Available from: http://www.pyrometer.com/paper0596.htm.
11. Minkina, W. and S. Dudzik, *Infrared Thermography : Errors and Uncertainties*. 2009, Chichester: John Wiley & Sons Ltd.
12. Boodhoo, K.V.K. and R.J. Jachuck, Process intensification: spinning disc reactor for condensation polymerisation. *Green Chemistry*, 2000. **2**(5): p. 235-244.
13. Wolfe, W.L. and G.J. Zissis, *The Infrared Handbook*. 1978: Office of Naval Research.
14. Boodhoo, K., Process intensification : spinning disc reactor for the polymerisation of styrene. *Ph.D. thesis*. 1999: University of Newcastle upon Tyne.
15. Wagner, C., Heat transfer from a rotating disk to ambient air. *Journal of Applied Physics*, 1948. **19**(9): p. 837-839.
16. Quinn, G. and B.M. Cetegen, Heat Transfer in an Evaporating Liquid Film Flowing Over a Rotating Disk. *Experimental Heat Transfer*, 2011. **24**(1): p. 88-107.
17. Woods, W.P., The hydrodynamics of thin liquid films flowing over a rotating disc. *Ph.D. thesis*. 1995: University of Newcastle upon Tyne.

APPENDIX 1– *Physical Properties of Therminol SP*

Temperature °C	Density kg/m³	Thermal Conductivity W/m.K	Heat Capacity kJ/kg.K	Viscosity Dynamic mPa.s	Viscosity Kinematic mm²/s**	Vapour pressure (absolute) kPa*
-10	892	0.132	1.798	308.6	346	-
0	885	0.131	1.834	143.3	162	-
10	878	0.130	1.870	73.8	84	-
20	872	0.128	1.906	41.6	47.70	-
30	865	0.127	1.942	25.2	29.10	-
40	858	0.126	1.978	16.3	18.99	-
50	852	0.125	2.013	11.1	13.05	-
60	845	0.124	2.049	7.90	9.39	-
70	838	0.123	2.085	5.90	7.02	-
80	831	0.122	2.120	4.50	5.43	-
90	825	0.120	2.156	3.56	4.32	-
100	818	0.119	2.191	2.88	3.52	-
110	811	0.118	2.227	2.38	2.93	-
120	804	0.117	2.262	2.00	2.49	-
130	797	0.116	2.297	1.71	2.14	0.1
140	790	0.115	2.333	1.48	1.87	0.2
150	783	0.113	2.368	1.29	1.65	0.3
160	777	0.112	2.403	1.14	1.47	0.5
170	770	0.111	2.438	1.02	1.32	0.7
180	762	0.110	2.474	0.91	1.20	1.1
190	755	0.109	2.509	0.82	1.09	1.5
200	748	0.107	2.544	0.75	1.00	2.2
210	741	0.106	2.579	0.68	0.92	3.0
220	734	0.105	2.614	0.63	0.85	4.1
230	726	0.104	2.649	0.57	0.79	5.5
240	719	0.103	2.684	0.53	0.74	7.4
250	711	0.102	2.719	0.49	0.69	9.8
260	704	0.100	2.755	0.45	0.64	12.8
270	696	0.099	2.790	0.42	0.60	16.6
280	688	0.098	2.825	0.39	0.56	21.3
290	680	0.097	2.860	0.36	0.53	27.2
300	672	0.096	2.896	0.33	0.50	34.4
310	663	0.094	2.932	0.31	0.47	43.1
320	655	0.093	2.967	0.29	0.44	53.7
330	646	0.092	3.003	0.27	0.42	66.3
335	642	0.091	3.022	0.26	0.40	73.6

* 1 bar = 100 kPa - ** 1 mm²/s = 1 cS

Note: Values quoted are typical values obtained in the laboratory from production samples. Other samples might exhibit slightly different data. Specifications are subject to change. Write to Solutia for current sales specifications.

Density (kg/m³) = 885.597 - 0.689367 * T(°C) + 1.9228 * 10^{-4} * T²(°C) - 8.87642 * 10^{-7} * T³(°C)

Heat Capacity (kJ/kg.K) = 1.83369 + 0.0036172 * T(°C) - 4.94238 * 10^{-7} * T²(°C) + 7.98115 * 10^{-10} * T³(°C)

Thermal Conductivity (W/m.K) = 0.131281 - 0.000114034 * T(°C) - 1.49876 * 10^{-5} * T²(°C) + 1.76622 * 10^{-11} * T³(°C)

Kinematic Viscosity (mm²/s) = $e^{\left(\frac{798.89}{T(°C)+97.7} - 2.65773\right)}$